

Modelling and simulation of variable speed pico hydel energy storage system for microgrid applications



Krishnakumar R. Vasudevan^{a,*}, Vigna K. Ramchandaramurthy^a, Gomathi V^b, J.B. Ekanayake^{c,d}, S.K. Tiong^c

^a Institute of Power Engineering, Department of Electrical Power Engineering, College of Engineering, Universiti Tenaga Nasional, Jalan IKRAM-UNITEN, 43000, Kajang, Selangor, Malaysia

^b Department of Electrical and Electronics Engineering, Anna University, Chennai, 600025, India

^c Institute of Sustainable Energy, Universiti Tenaga Nasional, Jalan IKRAM-UNITEN, 43000, Kajang, Selangor, Malaysia

^d Department of Electrical and Electronic Engineering, Faculty of Engineering, University of Peradeniya, Peradeniya, Sri Lanka

ARTICLE INFO

Keywords:

Pumped hydro storage system
Pico hydel energy storage system
Microgrid
Variable speed hydropower
Maximum power point tracking

ABSTRACT

The scheduling and dispatch of stochastic renewable energy sources can be difficult in a Microgrid (MG). Renewable energy sources can power the MG reliably if supported by energy storage systems, via hierarchical control of the MG. In this work, a sustainable energy storage system is modelled with the existing resources in an agricultural farm. The resource is a downscaled pumped hydro storage system called Pico Hydel Energy Storage System (PHESS). The PHESS is numerically modelled with the governing equations of various components in the system. The proposed configuration caters for the water demand of crops and the energy storage requirement in a renewable energy powered microgrid. A full scale power converter topology is employed for variable speed operation of the proposed energy storage system. The power absorbed from the microgrid and injected into the microgrid is controlled by adjusting the speed of PHESS. An adaptive perturb and observe algorithm is developed to control the storage system in the generating mode, thus enabling the maximum extraction of power at various discharge rates and hydraulic head. A relationship between the power and speed of the turbine is deduced through regression analysis to control the storage system in pumping mode. The proposed model of PHESS is optimized to accept power commands directly from the MG controller for various levels of controls in the MG thus ensuring plug and play feature. The results obtained from MATLAB/Simulink software justify the effectiveness of the control strategies in both modes of operation.

1. Introduction

India is a country with an intense population of 1.324 billion among which 304 million houses are yet to be electrified. National Energy Policy of India 2017 [1] aims to provide round the clock access to electricity by the year 2022. The agriculture sector contributes 16.4% to India's GDP [2], but the major population involved in agricultural activities live in remote villages. These villages are deprived of grid connection and solely depend on firewood, kerosene, diesel to meet their energy requirements. A possible solution to power the remote community is to develop reliable and resilient Microgrids (MG) with renewable energy sources. Firstly, ensuring reliable power supply with the stochastic renewable energy sources (RES) is a tedious task due to the high degree of uncertainty in power generation and demand. The reliability of the system is ensured by maintaining a power reserve of

5% to 10% of the total system capacity [3]. Secondly, a resilient microgrid has to recover from any contingency event, for that the high inertia provided by synchronous machines in a conventional grid has to be mimicked by an entity in the microgrid [4]. In a conventional power grid, the Pumped Hydro Storage System (PHSS) is used to store the humungous energy during the off-peak hours and inject power during the peak hours, black start. Similarly, energy storage systems are required in a microgrid to inject power during the low generation or high demand and absorb power during the high generation or low demand periods. The small scale solar PV or wind energy based microgrids primarily employ Battery Energy Storage System (BESS) to mitigate fluctuation in the power generation. But the BESS suffer from various drawbacks such as high life cycle cost, low lifecycle, frequent maintenance [5] and failures [6] as compared to PHSS. Achieving higher energy storage autonomy with BESS is a costly proposition compared to

* Corresponding author.

E-mail address: vasudevkrishna.ceg@gmail.com (V. Krishnakumar R.).

<https://doi.org/10.1016/j.est.2019.100808>

Received 23 January 2019; Received in revised form 28 May 2019; Accepted 17 June 2019

Available online 02 July 2019

2352-152X/ © 2019 Elsevier Ltd. All rights reserved.

PHSS which has higher energy density [7]. The PHSS, when operated with Battery Energy Storage System (BESS) offers optimal result in techno-economic comparison [8]. The feasibility of using PHSS and BESS in a system less than 30 kW has been analysed [9] and it was concluded that the PHSS has lower Cost of Energy (COE) than the BESS for lifetime greater than 10 years.

The conventional PHSS has various challenges such as flooding, rehabilitation of nearby communities and deterioration of the local ecosystem. To overcome the drawbacks mentioned, the capacity of PHSS can be downscaled to exploit its higher energy density for microgrid applications like the smaller pico hydel plants which are limited to 5 kW [10]. The smaller size of these plants has economic, environmental and operational advantages, unlike the large PHSS which are signalized by high capital investment, loss of biodiversity and long gestation period. The PHSS can be a superior energy storage option when the existing structures are used for storing the water. The use of abandoned open mines connected to an unconfined aquifer, nearby water streams, underground water source as the lower reservoir is reported previously [11–13]. There are about 8.78 million dug wells and 5.9 million shallow tube wells with an average depth of (20 m to 40 m) [14] which are in the agricultural farms of India. Water from these underground sources is pumped to a surface level tank which is used for irrigation of crops and domestic use. The farmers at the areas without the last mile grid connection rely on diesel generators to pump the water for irrigation. Approximately 8 lakh units are operating in agricultural fields of India. The use of renewable energy sources to power the pumps are a rising trend, where about 4000 and 1300 units of wind and solar powered pumps have been installed in the country respectively [14]. The configuration of a dug well and a surface level tank resembles a small scale Pumped Hydro Storage System (PHSS) which has no upfront capital cost for construction of reservoirs. The configuration can be used to solve a bi-folded objective of water pumping and store electrical energy produced by renewable energy sources. The system is termed as Pico Hydel Energy Storage System (PHESS) as its capacity is limited to 5 kW.

The variable speed operation of PHSS in generating mode offers improved efficiency, instantaneous active power injection and wide operating region. Whereas in pumping mode, the variable speed operation allows part load operation and active power control [15]. The suitable choice of machine, power electronic topology, and control strategies play a vital role in reliable variable speed operation of PHESS. There are different topologies developed for variable speed hydel generation, employing Current Source Converter (CSC) and Voltage Source Converter (VSC) instrumenting various machines [16–20]. A Permanent Magnet Synchronous Machine (PMSM) which has advantages over Doubly Fed Induction Machine (DFIM) [21] is coupled to Reversible Pump Turbine in this work. It is also possible to control the synchronous machine with back to back VSCs but it requires field control loop to adjust the excitation of the field windings [22]. The review of converter-fed PMSM for a hydel generation would lay a foundation to derive the control strategies for the proposed system. As the power only flows from machine to the grid in a pico hydel generation scheme it possible to use unidirectional converters for the power conversion with the simple control mechanism. The unidirectional power converter topology for hydel generation includes an uncontrolled rectifier, DC-DC converter and a Voltage Source Inverter (VSI) in which the speed of the PMSM is controlled by the DC-DC converter [23,24]. Another unidirectional converter topology employs an uncontrolled rectifier and a Z source inverter [25]. The back to back Voltage Source Converters (VSC) for power generation were widely used in pico and micro-hydro plants [26–29].

In the recent past, pico hydel generation has been utilized to power the most underprivileged economies of the world which include rural areas and the remote villages. However, the operation and control of pico hydel units as an energy storage system was not extensively researched. The bidirectional power flow property of back to back VSC is

utilized to operate the proposed PHESS in generating and pumping modes of operation in this work. Effective control of the power converter determines the efficiency of the storage system and the stability of the microgrid. The vector control strategies provide better dynamic response than scalar control for converter fed PMSM. Among the vector control strategies, the Field Oriented Control (FOC) responds to fast changes in load torque variations than the Direct Torque Control (DTC) [30]. The DTC has high current harmonics and high ripple content in the real and reactive power due to high switching frequency and hysteresis current controllers [31]. Efficient estimation of reference rotor speed in pumping as well as generating mode is required for the FOC to control the speed of PMSM. A single reference speed estimation algorithm cannot be used for both the modes as the principles of control differ. So, the speed reference should be estimated separately and appropriately in generating and pumping modes of operation.

In the generating mode, variable speed control techniques aim to extract maximum power from the turbine for various water discharge rates which also widens the operating region of the turbine. The Maximum Power Point (MPP) algorithms applied to PHSS are categorized as direct and indirect methods. The indirect methods use an exact mathematical model of the turbine to estimate the speed reference whereas the direct methods do not require information about the turbine model. An indirect method based on a power-speed lookup table derived from the turbine hill chart has been used to control the DFIM based variable speed hydel plant [15]. The Perturb and Observe (P&O) algorithms based on the hill climbing technique is one of the popular direct methods employed in wind energy and solar PV systems. A P&O algorithm was used to control variable speed micro-hydro systems [28] which used a fixed step size to track the maximum power. The fixed step P&O algorithm with a small step size has a sluggish response with low oscillations around the MPP, whereas the use of large step size to achieve rapid response results in sustained oscillations around the MPP. To overcome these issues, a variable step size based on toggling between upper and lower limits has been proposed in [29,32]. The algorithm toggles between the extremities which can induce vibrations on the turbine shaft. In another work, a gradient descent method based on the efficiency-current gradient was proposed to control the speed of the small hydel plant using unidirectional converter topology [23], which is not suitable to control the VSC in the conceived system. The advanced computational intense intelligent algorithms like Artificial Neural Network and Model Predictive Controls have been proposed for hydropower plants with DFIM [33–35]. To address the issues in fixed step P&O algorithm and to offer a simple control technique, an Adaptive Perturb and Observe (APO) algorithm based on the power-speed gradient is proposed in this work.

In pumping mode, the objective of the speed control strategy is to utilize minimum available surplus power in the microgrid to pump the water to the upper reservoir. The pumping operation of PHESS is similar to the wind and solar pumping systems but the key difference is the bidirectional property of the proposed system opposed to unidirectional power flow water pumping systems. Conventionally a diode bridge rectifier on the grid side and a VSC on the machine side is used to control the power input to the water pumping system and hence achieve variable speed pumping [36]. In the renewable water pumping systems, the speed reference is computed with the governing equations of the electrical machine and the maximum power command from the MPPT algorithm of the source [37–39]. In another work, the speed reference is derived from the DC link voltage control loop using a PI controller [40]. The reported works do not consider the hydraulic pump characteristics governed by affinity laws [41] to derive the speed reference. To achieve satisfactory pumping with partial electric power input to the machine, the speed reference is estimated by forming a relationship between the speed and the available surplus power in the microgrid through regression analysis. The analysis is carried out by considering the pumping head and discharge rate defined by the affinity laws of the centrifugal pump.

Thus, the contribution of this paper is as follows:

- i A sustainable energy storage system is modelled with the existing dug well and a surface level tank used for irrigation in the agricultural fields of rural India.
- ii The sizing of the upper reservoir is done based on the autonomy required with the physical size constraint and an optimal operational flow chart of the reservoir model is presented.
- iii An Adaptive Perturb and Observe algorithm based on power–speed gradient is proposed to extract maximum power from the reversible pump turbine at various discharge rates in generating mode of PHESS.
- iv A relationship is established between the surplus power in the microgrid and speed of the reversible pump turbine using the Affinity Laws of centrifugal pumps through regression analysis, to estimate the speed reference in pumping mode.
- v The developed strategies are used to derive the reference values for Field Oriented Control of PMSM in generating, pumping modes and its effectiveness is discussed with the simulation results obtained in MATLAB/Simulink.
- vi The control techniques proposed in this work are optimized to plug the PHESS into a microgrid with any type of renewable energy source. Since it is modelled and controlled independently of the source. The system has the capability to accept direct power commands from the microgrid controller to ensure plug and play operation. The fast response of the PHESS by variable speed operation and higher energy storage autonomy with the upper reservoir makes the proposed system to take part in primary and secondary control of microgrid.

The next section describes the proposed energy storage system followed by the system component modelling in section 3. The proposed reference speed estimation techniques, the Field Oriented Control of power converters are elaborated in section 4 and 5 respectively. The performance of the system with the proposed control strategies under generating and pumping modes are discussed with the results obtained from MATLAB/Simulink in section 6.

2. Proposed pico hydel energy storage system

There are two schemes of PHSS, namely mixed PHSS which have natural inflow and pure PHSS [3] whose discharge operation (generating) depends on the volume of water pumped by the pumping system during the previous charging cycle (pumping). The Pico Hydel Energy Storage System (PHESS) developed in this work is similar to the pure PHSS since the total power generation depends on the water pumped in the previous cycle. The functional block diagram of the proposed PHESS is shown in Fig.1. The upper reservoir is a surface level tank and the lower reservoir is a dug well used for irrigation of agricultural crops. The Microgrid (MG) controller acts as a master control which sends power command to the speed controller and the hydraulic governor. The hydraulic governor is used to regulate the water flow into the inlet pipe based on its power command and the speed controller extracts maximum power from the hydro turbine. A single Reversible Pump Turbine unit coupled to a Permanent Magnet Synchronous Machine is employed in this system to generate power and pump water to the upper reservoir. The PHESS operates as a hydropower plant in the generating mode and acts as a large capacity energy storage system in the pumping mode. The bidirectional power flow is controlled by a pair of back to back VSC. The dual mode operation of PHESS is further explained in the next subsection by comparing it with the BESS, without considering the characteristic difference between them.

2.1. Modes of operation

2.1.1. Pumping mode

During the off-peak hours, when there is surplus power in the microgrid, the frequency of the microgrid increases beyond the nominal value. To curtail the frequency deviation, either the power has to be absorbed by a storage system or the generation has to be limited. It is uneconomical to limit the renewable power generation when there is an availability of acceptable wind speed or solar insolation, so the excess power can be stored in the PHESS. The surplus power in the microgrid is absorbed by the electrical machine coupled to the reversible pump turbine and operates as a motor. The RPT unit pumps water from the lower reservoir to the upper reservoir and stores the electrical energy as the potential energy. This mode of operation is analogous to the charging cycle of the BESS.

2.1.2. Generating mode

When the microgrid has a deficit of power due to high demand in peak hours or due to unavailability of natural resources, the frequency of the microgrid drops as the demand for electrical energy increases. The energy storage systems will be called in for primary frequency support and it has to provide its service. The deficiency in power can be met with the PHESS operating in generating mode like a conventional hydropower plant. The quantum of deficit power is provided by the Microgrid controller, and the gate valve is adjusted accordingly to regulate the water flow. The potential energy stored in the upper reservoir as the difference in the head is converted into electrical energy when the water impinges on the Reversible Pump Turbine coupled to PMSM. The water after exerting the force on the turbine is collected and stored in the lower reservoir. This mode of operation is congruent to the discharging cycle of the BESS.

2.2. Variable speed pico hydel energy storage system

The large capacity fixed speed pumped hydro storage system does not offer flexibility to adjust its power input based on the grid requirements in pumping mode and the narrow operating head deviation limits its operation in generating mode. The flexibility of such large units in pumping mode is increased by using several small-sized pumps to obtain a stepped control. In generating mode, the fixed speed PHSS are optimized to operate around its synchronous speed with rated head and discharge rates. As the head varies, the discharge of water is adjusted by the hydraulic governor to maintain the synchronous speed and the unit is shut off when the head falls below a minimum value [33]. In the case of considered small capacity PHESS, it is desirable to utilize the entire volume of water stored in the upper reservoir to achieve the desired autonomy. To do so, the RPT should be optimized for the lowest possible value of head, as the dependence of turbine speed on the operating head is even more pronounced in the proposed PHESS due to the large variation in the head. Whereas in pumping mode, the power input to the reversible pump turbine has to be continuously varied to operate it with the minimum excess power available in the microgrid instead of operating it at rated power. The above issues can be addressed by the variable speed operation of PHESS so that the instantaneous supply and demand of the isolated MG can be effectively maintained in both the modes of operation.

3. Modelling of hydraulic system

3.1. Design and sizing of reservoir

The reservoirs of PHESS are indistinguishable with battery. The State of Charge (SoC) of the battery is correlated with the amount of water in the reservoir in the various literature [5,8]. In this work, the upper reservoir is kept at the ground level and an open well is utilized as the lower reservoir. The design of the upper reservoir is mainly based

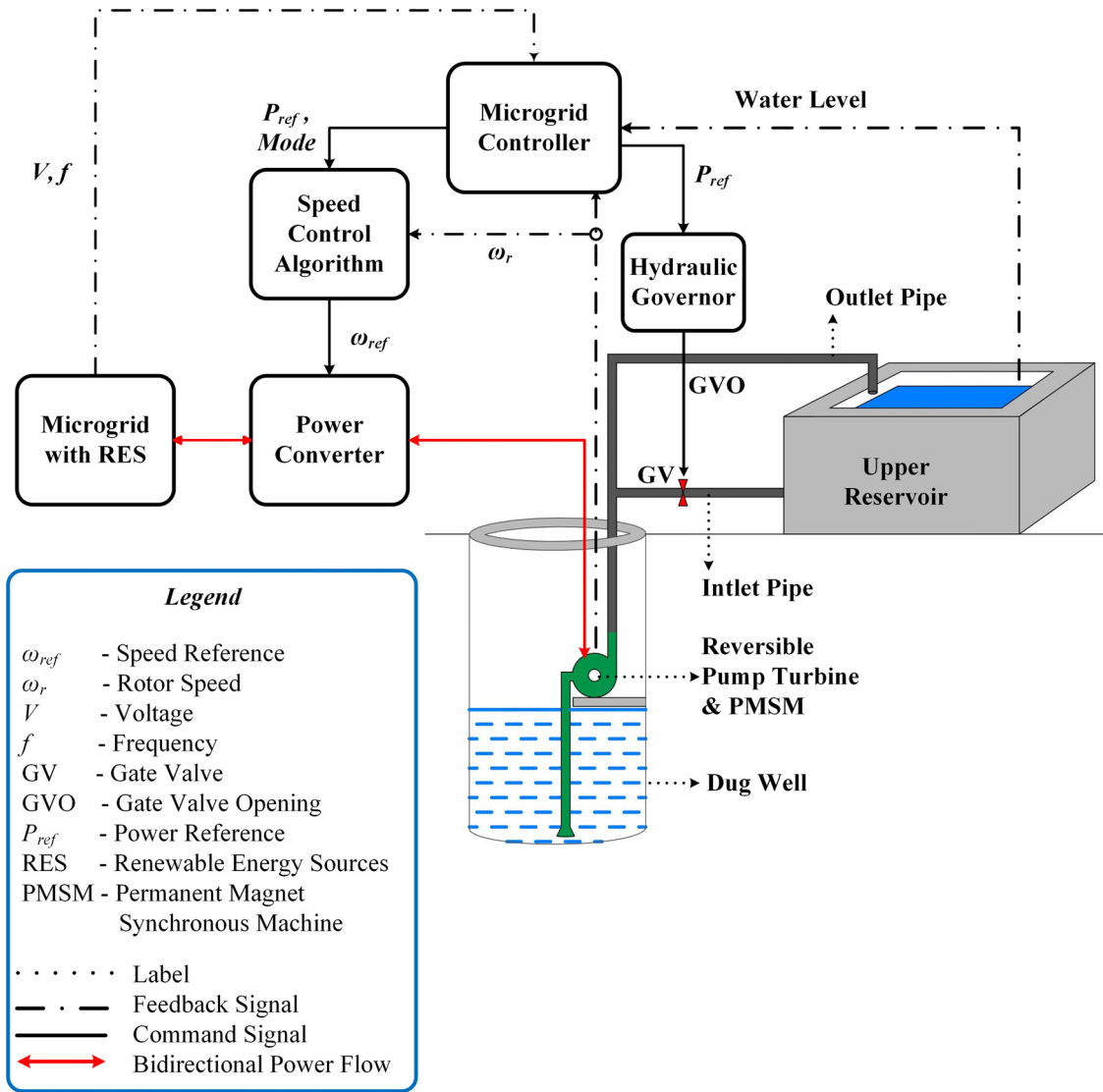


Fig. 1. Functional block diagram of the proposed PHESS with dug well.

on the required autonomy of energy storage. The volume of the reservoir is directly proportional to the autonomy which is the maximum duration the PHESS can deliver the rated power. Similar to conventional hydropower plants the hydraulic head H [10] is calculated at any point with Eq. (1).

$$H = z + \frac{p}{\rho g} + \frac{v^2}{2g} \quad (1)$$

Where z is the elevation, p is the pressure of the water in the conduit, v is the velocity of the water jet, ρ is the density of the water, and g is the acceleration due to gravity. The volume of the reservoir can be calculated with the autonomy required and is given by Eq. (2).

$$V = \frac{(3.6 \cdot 10^6) n_d E_l}{\eta_t \rho g H} \quad (2)$$

Where, n_d , E_l , η_t , H are autonomy, electrical load, the acceleration due to gravity and head respectively. The value of $n_d = 5$ h is chosen based on the physical size limitation of the upper reservoir. The value of net head $H = 17$ m is chosen based on the average depth of dug wells (20 m–40 m) in India [14] and $E_l = 1.1$ kW is assumed. The parameters are used to determine the water storage capacity of the upper reservoir.

$$V = \frac{3.6 \cdot 10^6 \cdot 5 \cdot 1.1}{0.9 \cdot 1000 \cdot 9.81 \cdot 17} = 132 \approx 150 \text{ m}^3$$

The dimensions of the reservoir are computed by fixing the height of the reservoir to 5 m as the operational head of the selected turbine varies from 16 m to 22 m. The length and breadth of the reservoir are computed with the length to breadth ratio of 1.2:1. The computed dimensions of the reservoir are $height = 5$ m, $length = 6$ m, $breadth = 5$ m.

The change in reservoir water level can be computed using Eq. (3).

$$\Delta H = \frac{Volume - \int Q dt}{length \cdot breadth} \quad (3)$$

The net head after 1 s is computed by substituting the net volume and dimensions of the reservoir, the rated discharge computed with the Eq. (5).

$$\Delta H = \frac{150 - (15 \cdot 10^{-3} \int dt)}{6 \cdot 5} \quad (m)$$

Therefore, $\Delta H = 4.9995$ m

The net change in the head after a second is, $H_d = 5 - 4.9995 = 5 \cdot 10^{-4}$ m

The change is so minimal and it takes approximately 30 min for a 1 m change in head. Hence, the reservoir model has to be scaled down if

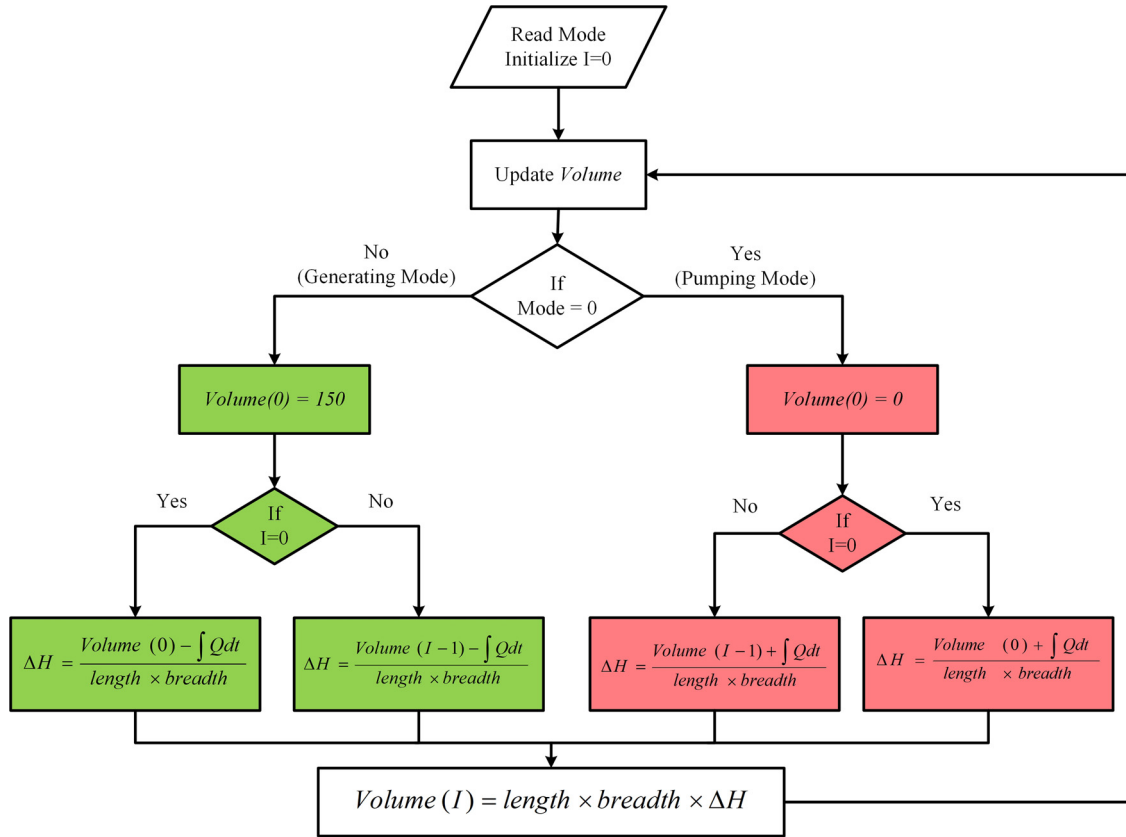


Fig. 2. Operational flow chart of the upper reservoir.

it is necessary to run the simulation to fully empty the reservoir or fill the reservoir up to the brim with water. The operational flowchart of the upper reservoir is presented in Fig.2. *Mode 1* represents the operation of PHESS in generating mode, in which the reservoir level and volume have to decrease linearly with time. *Mode 0* indicates the operation of PHESS in pumping mode, during which the reservoir level and volume increase linearly with time. In both the modes of operation, the slope of the curve is dictated by the discharge of water (Q) in m^3/s at that time interval.

3.2. Modelling of reversible pump turbine

There are various hydraulic turbines used in low head applications and thirteen of them are reviewed in the literature [42]. The hydro turbines are broadly classified as impulse and reaction turbines. Conventionally, the hydro turbine is chosen based on its specific speed, operating head, output power, and the shaft speed. The propeller turbines were used for low head applications due to its low cost and simple and rigid construction. The application of turgo turbines for the low head operation is analysed [10] and is proven to have better-operating efficiency than the propeller turbine. But the use of those turbines requires a separate machine to pump the water. To save the capital cost, a single reversible pump turbine can be used for both the modes of operation [43]. The water hammer effect and the elasticity of the water column have been neglected, the dynamic equations are linearized for modelling the RPT. The process of modelling the turbine is a continuation of the reservoir model presented in the last section. The jet head of the turbine as a function of time is calculated by the Eq. (4). The jet head $H_j(t)$ is the difference in height between the rotational axis of the turbine and the reservoir level at that instant.

$$H_j(t) = C_v^2 H_n(t) \quad (4)$$

Where, $C_v = 0.97$ is the coefficient of velocity and it is defined as the

ratio of the actual velocity of the jet to the theoretical velocity [10] and $H_n(0) = 17m$ is the net operating head of the Reversible Pump Turbine (RPT) which is a function of time.

$$\text{Therefore, } H_j(t) = 0.97^2 \cdot 17 = 16 \text{ (m)}$$

The rated discharge of water Q_t in m^3/s is calculated from Eq. (5),

$$Q_t = \frac{\text{Volume of Upper Reservoir}}{\text{Total Time of Discharge}} \quad (m^3/s) \quad (5)$$

The efficiency of the RPT is the function of rotor speed ω , the jet head H_j and the guide vane position γ [44] which is given by Eq. (6)

$$\eta_t(\omega, \gamma, H_j) = \frac{P_t}{\rho g H_j(t) Q_t} \quad (6)$$

The total output of the turbine shaft is the product of the efficiency of the turbine η_t , and the hydraulic power input to the turbine, where $\rho = 1000 \text{ kg/m}^3$ is the density of water.

$$P_t = \eta_t \rho g Q_t H_j(t) \text{ (W)} \quad (7)$$

The shaft torque of the turbine is obtained with its relationship between power and speed given by equation (8).

$$T_s = \frac{P_s \times 60}{2\pi N} \text{ (Nm)} \quad (8)$$

But the instantaneous torque is computed by taking the speed feedback from the machine since both the turbine and PMSM are connected to the same shaft.

The power input to the RPT in pumping mode is given by the Eq. (9),

$$P_p = \frac{\rho g Q_p H_p}{\eta_p} \quad (9)$$

Where the pumping head H_p remains constant at 17 m, Q_p is the pump discharge and η_p is the efficiency of RPT in pumping mode.

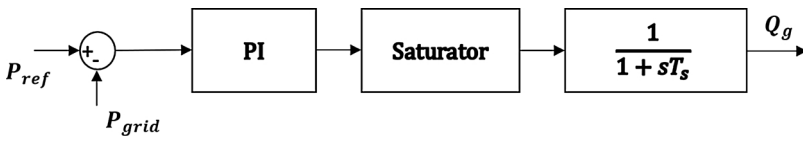


Fig. 3. Model of the Hydraulic Governor with PI Controller.

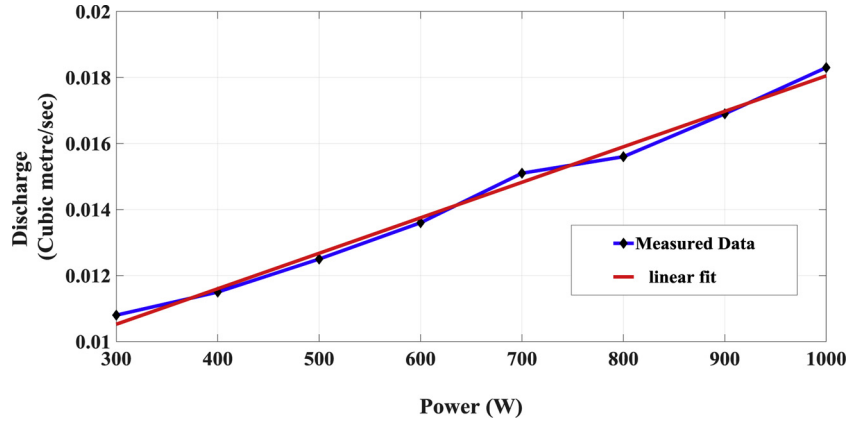


Fig. 4. Power Vs Discharge Characteristics obtained through linear regression analysis.

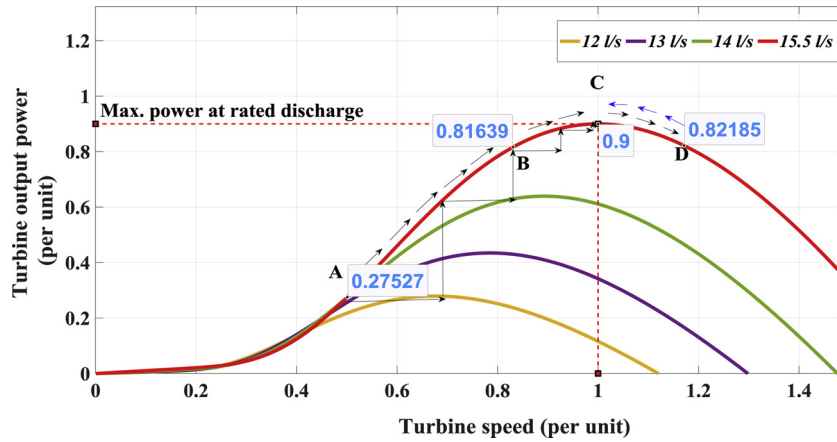


Fig. 5. Power Vs Speed characteristics of the reversible pump turbine.

3.3. Modelling of hydraulic governor

The water discharge in the conduit is controlled by the gate valves operated by servo motor. The gate valve position command is given by the hydraulic governor. The hydraulic governor takes reference power as input from the microgrid controller. The control diagram of the hydraulic governor is shown in Fig. 3. The hydraulic governor should respond to the change in reference power command. The PI controller is tuned to adjust the servomotor position (gate valve position) based on the difference between P_{ref} and P_{grid} , to vary the water discharge (Q_g) at that particular interval

The modelling of the hydraulic governor is validated by plotting the data points on a 2D graph and carrying out a regression analysis. The discharge is a dependent variable hence it is plotted on the Y-axis and the independent variable power is plotted on the X-axis as shown in Fig. 4 and MATLAB curve fitting toolbox is used to find the best fit. The best fit is found by analysing the Root Mean Square Error (RMSE) value and the linear fit has the lowest RMSE value than higher degree polynomial fit. Hence, it validates the linear relationship between the power and the discharge, which is explained in the previous section Eq. (7).

4. Reference speed estimation

The hydropower plants operate at a synchronous speed corresponding to the fundamental frequency of the grid. The variable speed technology was initially employed to extract maximum from wind electric system which used DFIM and PMSM for power generation. In both cases, the speed of the machine is controlled by the power converters which obtains its reference speed value from different MPPT techniques [45]. A similar concept can be used to develop separate control strategies in pumping and generating modes of PHESS. The principal aim of the developed strategies is to estimate the reference rotor speed for optimal performance of PHESS in both the modes. An Adaptive Perturb and Observe algorithm based on the power-speed gradient is developed to estimate the rotor reference speed in generating mode. A relationship between the power and the speed of the chosen RPT is established through regression analysis to estimate the reference speed in pumping mode.

4.1. Reference speed estimation in generating mode

The rotor speed reference is obtained by using an Adaptive Perturb and Observe (APO) algorithm. The power versus speed characteristics of the reversible pump turbine is shown in Fig.5, which is a family of

curves obtained for different levels of discharge and the characteristics are used to develop the reference estimation algorithm. The proposed APO algorithm has a dual objective, the first is to achieve rapid tracking of MPP based on the hydraulic conditions of the system and the second objective is to minimize the oscillations induced in the shaft during the speed tracking. In the proposed APO algorithm, the rotor speed is varied about its initial operating point and the power output is measured to make the speed change decision in the next sampling time. The estimated reference speed $\omega_{ref(g)}$ is given by Eq. (10) which depends on the sign of power change and the adaptive step size k . The change in power and speed with respect to the previous sample is given by Eqs. (11,12)

$$\omega_{ref(g)} = \begin{cases} \omega_{i-1} + abs(k\Delta\omega) \text{ if } \Delta P_s > 0 \\ \omega_{i-1} - abs(k\Delta\omega) \text{ if } \Delta P_s < 0 \end{cases} \quad (10)$$

$$\Delta P = P_i - P_{i-1} \quad (11)$$

$$\Delta\omega = \omega_i - \omega_{i-1} \quad (12)$$

As the step size plays a crucial role in the performance of the MPPT algorithm, the factor k is decided based on the gradient of the turbine operating curve. When the power gradient is steep the value of k is high and when the search approaches the MPP the curve becomes almost flat which lowers the value of k as shown in Eq. (13).

$$k = \frac{\Delta P}{\Delta\omega} \quad (13)$$

$$\Delta P_s = \text{sgn}(\Delta P) = \begin{cases} -1 & \Delta P < 0 \\ 0 & 0 \leq \Delta P \leq 0.05 * P_{nom} \\ 1 & \Delta P > 0 \end{cases} \quad (14)$$

To explain the algorithm, the curve shown in red colour which corresponds to the rated discharge of 15.5 l/s is used. The desired operating point of the turbine is C which is the maximum power point (MPP) at the rated discharge rate and the MPP vary for different rates of water discharged to the turbine. The search for MPP starts from the initial operating point A, the speed is increased based on the value of k and the power is measured. The sign of change in power ΔP is extracted by using a signum function given by Eq. (13). If the value of ΔP_s is 1 then the search for MPP is continued in the same direction by increasing the reference speed by $k\Delta\omega$. Once the point B is reached the value of ΔP_s is still 1, so the search for MPP is continued in the same direction by accelerating the turbine.

After reaching point C, the value of ΔP_s becomes zero but to make sure that the reached MPP is correct, the reference speed is increased further. The acceleration of the turbine pushes the operating point D, at that point the power is lower than the previous sample value which makes the value of ΔP_s as -1. Due to the negative change in power, the rotor is decelerated and the system finally settles at point C as long as

the discharge value remains constant at 15.5 l/s.

4.2. Reference speed estimation in pumping mode

In large PHSS, the RPT can satisfactorily pump the water from the lower reservoir with 70% of its rated power [3] thus providing flexibility up to 30% of the rated power. So, it is possible to control the power drawn by the RPT by adjusting the speed of the machine by optimizing the part load pumping operation of RPT. The operation of the RPT in pumping mode is governed by the Affinity Laws for centrifugal pumps [41] which establishes the relationship between the water discharged to the pump and speed of the pump (15), pumping head and speed of the pump (16).

$$\frac{Q_1}{Q_2} = \frac{N_1}{N_2} \quad (15)$$

$$\frac{H_1}{H_2} = \frac{N_1^2}{N_2^2} \quad (16)$$

According to Eq. (9), the discharge of the RPT is directly proportional to its power input and by Eq. (15) the discharge is proportional to speed. In pumping mode as the head remains constant, Eq. (16) is neglected. Thus the speed of operation can be varied in accordance with the power input to the RPT and it necessitates to form a relationship between the rotor speed and the surplus power in the microgrid. The relationship is formed by collecting the data points and performing a statistical regression analysis. To collect the data points, the mechanical torque acting on the shaft of the RPT is maintained constant as the pumping head remains constant. The power input to the PMSM is varied throughout its operating region by controlling the switches of the Machine Control Converter (MCC) which acts as a Voltage Source Inverter (VSI) and the rotor speed is sensed. The regression analysis is performed by defining the response and predictor variables. The rotor speed of the RPT depends on the electrical power input to the PMSM. So, the rotor speed is defined as the response variable and the electrical power input to the PMSM is defined as the predictor variable. The analysis is performed with almost 150 data points collected throughout the operating region of the PMSM by varying its input power. The values are plotted in a 2D X-Y plot since there are only one predictor and one response variable. The analysis is carried out by using MATLAB curve fitting toolbox and the equations for linear, quadratic and cubic fit have been obtained and the plot is shown in Fig. 6.

To find the best fit, the norm of residuals is used as a measurement index in this analysis. The equations and norm of residuals for linear, quadratic and cubic fit are given in Table 1. The lower value of the norm of residuals determines the best fit. The norm of residuals plot is shown in Fig. 7 and the value for cubic fit 45.43 is lower than the quadratic and linear fit. Hence the obtained cubic polynomial (17) is

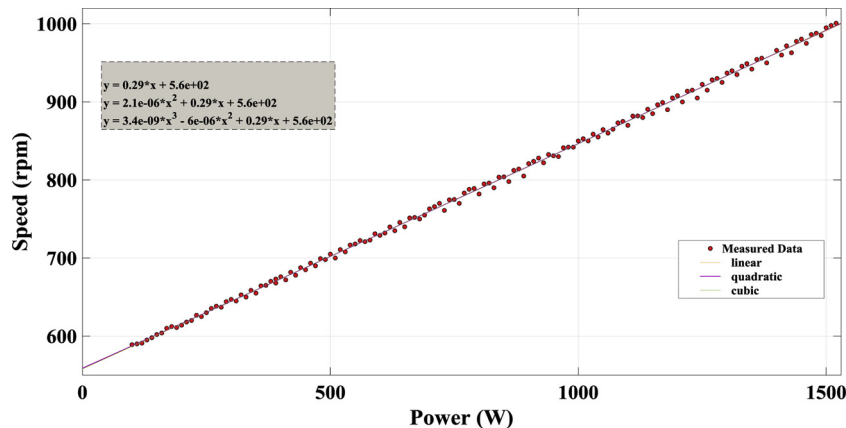


Fig. 6. Curve Fitting plot of the regression analysis.

Table 1
Curve fitting parameters and equation of various techniques.

Fitting Method	Equation	Norm of Residuals
Linear	$W_{ref} = 0.29 \times P_e + 560$	45.6461
Quadratic	$W_{ref} = 2.1 \times 10^{-6} \times P_e^2 + 0.29 \times P_e + 560$	45.4852
Cubic	$W_{ref} = 3.4 \times 10^{-9} P_e^3 - 6 \times 10^{-6} \times P_e^2 + 0.29 \times P_e + 560$	45.4309

used to estimate the reference rotor speed. A similar equation was framed in [46] for a variable speed PHSS.

$$\omega_{ref(p)} = 3.4 \times 10^{-9} P_e^3 - 6 \times 10^{-6} \times P_e^2 + 0.29 \times P_e + 560 \quad (17)$$

5. Power electronic control

With the advent of modern power semiconductors, full-scale converter topology is widely used for variable speed operation of the pumped hydro storage system. The power converter topology and the control blocks of the proposed PHESS are shown in Fig. 8. A pair of Voltage Source Converters (VSC) are used to control the speed of PHESS and the direction of power flow. In generating mode, the Machine Control Converter (MCC) acts as an active rectifier and the Grid Coupling Converter (GCC) operates as a Voltage Source Inverter (VSI). Whereas in the pumping mode of operation the PHESS has to draw power from the grid, so the operation of VSCs is interchanged. The MCC is operated as a VSI and the GCC is operated as an active rectifier. There are well-established techniques to control the PMSM which include scalar and vector control on a broader spectrum. The Field Oriented Control (FOC) which is a subclass of vector control is used to generate the reference values for Space Vector Pulse Width Modulation (SVPWM). The control of PMSM is carried out in the synchronously rotating frame by decomposing the stator currents and voltages into d - q components by Park's Transformation. To control the flux and the torque of PMSM independently, the stator current vectors are decomposed into i_{sd} and i_{sq} components respectively. The FOC allows the control of the flux and torque of the PMSG separately, by using a cascaded speed and current control loop with Proportional Integral (PI) controllers.

5.1. Machine control converter

The speed control of PMSM in pumping mode and generating mode is achieved by adjusting the firing pulses to the MCC. The control strategy employed in both the modes of operation of PHESS is the same whereas the vital distinction lies in the estimation of the reference rotor

speed which was discussed in the previous sections. The speed control principle of PMSM is explained with the dynamic torque equation of rotating machines (18). In Eq. (18) T_h is the Mechanical torque delivered by the reversible pump turbine, T_g is the Electromagnetic torque of the generator, J is the Inertia of the turbine ω_m is the rotor speed. The Eq. (18) shows that the rotor speed can be controlled by changing the electromagnetic torque which depends on the q-axis current component. To accelerate the machine T_g has to be reduced so that the difference between T_g and T_h increases. To decelerate the machine T_g has to be increased so that the difference between T_g and T_h decreases.

$$T_h = T_g + J \frac{d\omega_m}{dt} \quad (18)$$

The control architecture of the MCC in the synchronously rotating reference frame (d - q) is shown in Fig.9. The difference between the actual and the reference speeds is fed as input to the speed controller whose output is the q-axis reference current component $i_{s,q}^*$, which is further fed to the q-axis current controller and the required q-axis stator voltage $U_{s,d}$ is generated. The d-axis reference current component $i_{s,d}^*$ is made zero to keep the flux independent of the control strategy. The negated value of d-axis current component $i_{s,d}$ is the input to the d-axis current controller, which gives d-axis stator voltage $U_{s,d}$.

$$U_{s,d}^* = U_{s,d} - \omega L_s + V_{s,d} \quad (19)$$

$$U_{s,q}^* = U_{s,q} + \omega L_s + V_{s,q} \quad (20)$$

Decoupling terms are added to the difference in actual and reference dq components of the stator voltage, to have a better dynamic response and the required values of the stator voltage vector $U_{s,d}^*$, $U_{s,q}^*$ are produced as shown in Eqs. (19,20) respectively. The obtained d - q components are converted to $\alpha\beta$ components by Clarke's Transformation. Finally, Space Vector Pulse Width Modulation (SVPWM) technique is used to generate the gate pulses based on the desired reference voltages.

5.2. Grid coupling converter

The operation of Grid Coupling Converter (GCC) focuses on the control of active, reactive power delivered to the grid in both the modes of PHESS, grid synchronization and the power quality [47] The control strategy of GCC in the d - q reference frame has cascaded structure to control the grid current, reactive power and the DC link voltage as shown in Fig.10.

The faster acting inner loops ensure the power quality and its performance can be improved with harmonic compensation. The voltage loop regulates the active power flow of the system by maintaining the DC link voltage and reactive power delivered to the grid. It is evident from the forthcoming Eqs. (21–24) that the active and reactive power delivered to the grid or drawn from the grid can be controlled by

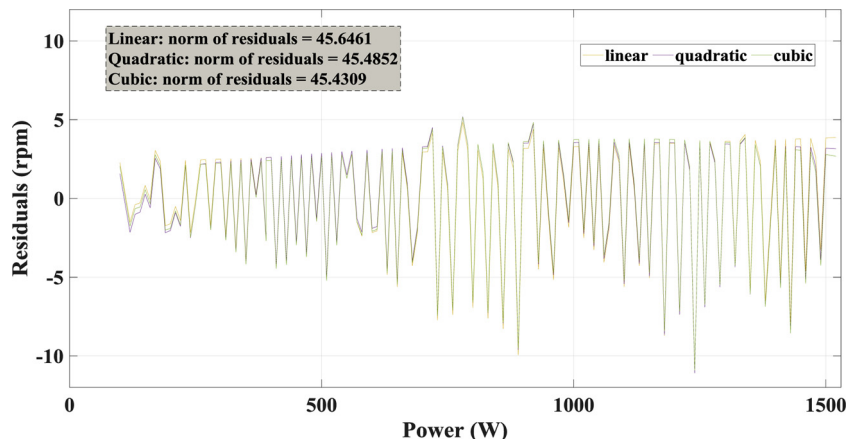


Fig. 7. Norm of Residuals plot for various fitting techniques considered.

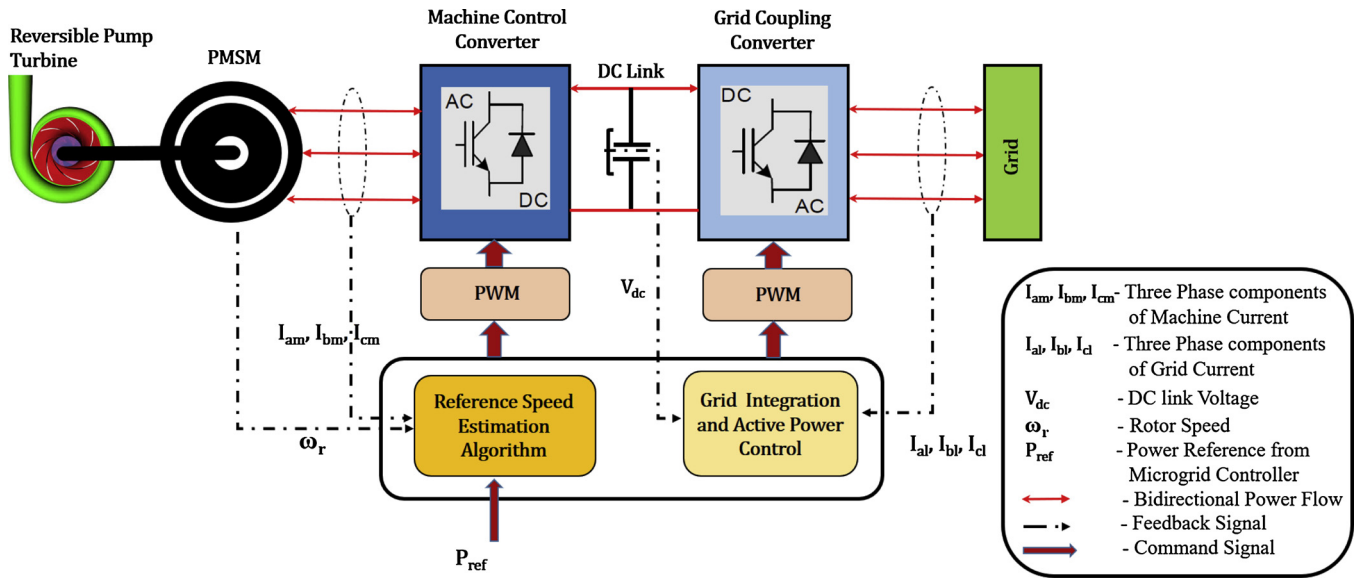


Fig. 8. Control architecture of PHESS with Full Scale Power Converter Topology.

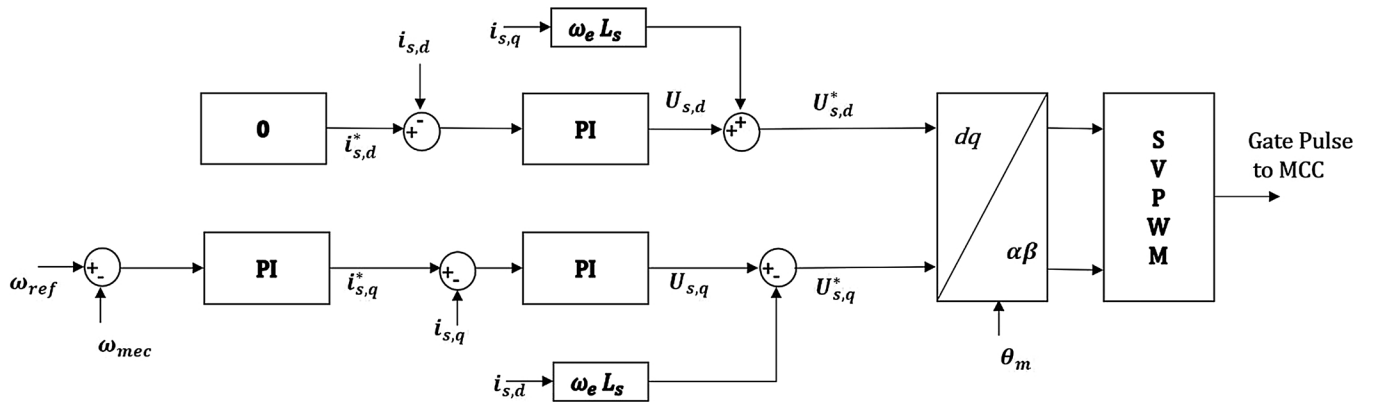


Fig. 9. Control strategy of Machine Control Converter in the d-q reference frame.

changing the respective components of the inverter current. The quantum of real and reactive power is controlled based on the command from the MG controller.

$$P = \frac{3}{2} v_{g,d} i_{g,d} \quad (21)$$

$$P = -\frac{3}{2} v_{g,d} i_{g,d} \quad (22)$$

$$Q = \frac{3}{2} v_{g,d} i_{g,q} \quad (23)$$

$$Q = -\frac{3}{2} v_{g,d} i_{g,q} \quad (24)$$

The following Eqs. (25) and (26) gives the instantaneous active and reactive power.

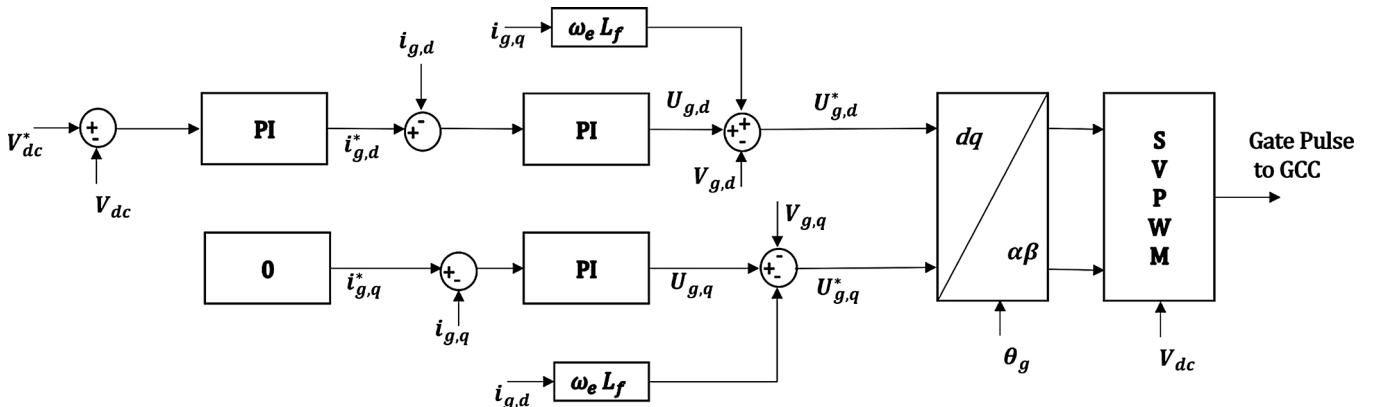


Fig. 10. Control strategy of Grid Coupling Converter in the d-q reference frame.

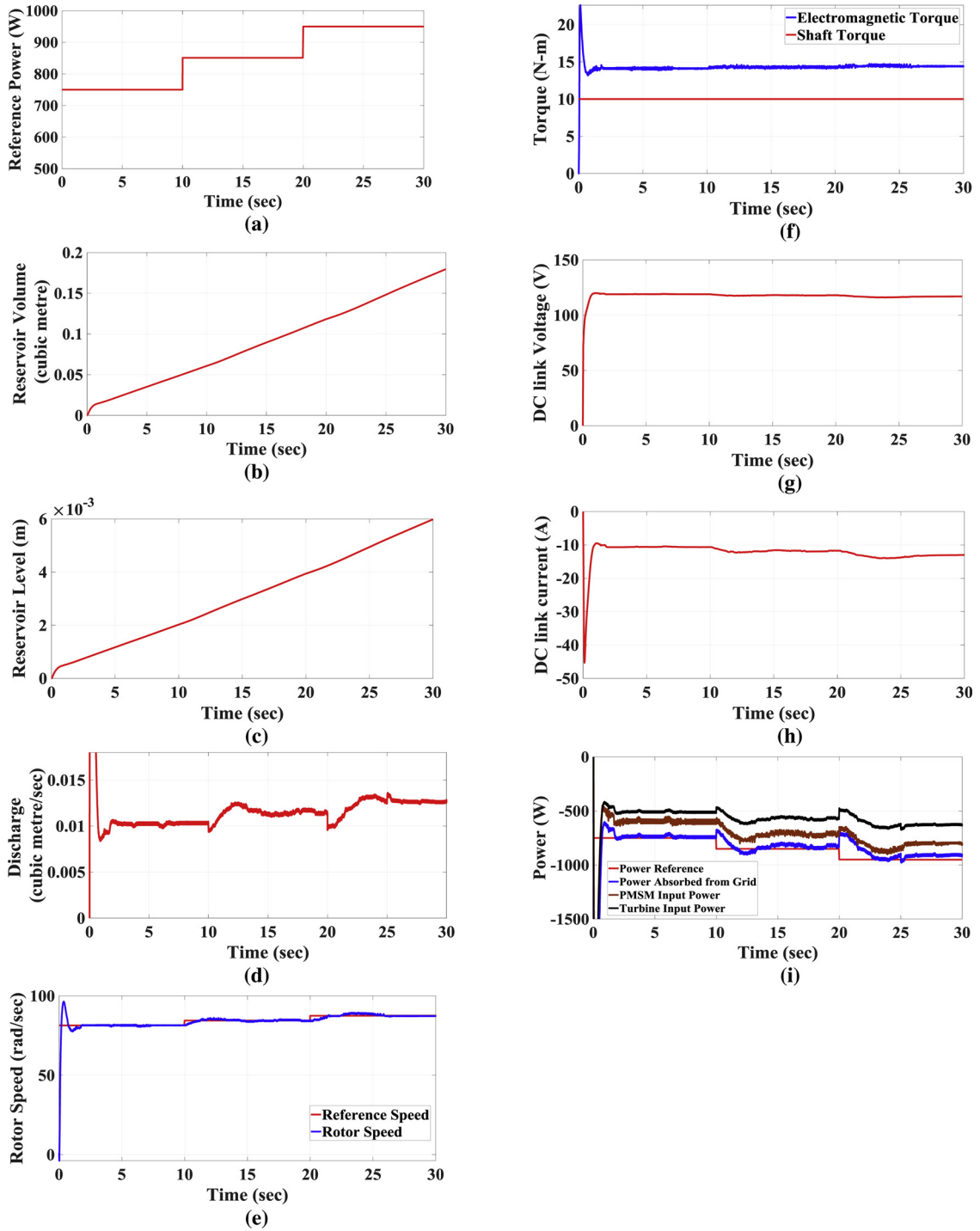


Fig. 11. Analysis of Pumping Mode with the obtained simulation results: (a) Reference power command from MG controller (b) Increase in Reservoir Volume (c) Increase in Reservoir Level (d) Water discharged by RPT (e) Mechanical Shaft Speed (f) Electromagnetic & Shaft Torque (g) DC link Voltage (h) DC link Current (i) Power measured at various points.

$$P(t) = \frac{3}{2} (V_{g,d}(t)i_{g,d}(t) + V_{g,q}(t)i_{g,q}(t)) \quad (25)$$

$$Q(t) = \frac{3}{2} (-V_{g,d}(t)i_{g,q}(t) + V_{g,q}(t)i_{g,d}(t)) \quad (26)$$

The total power flow into the DC link capacitor is given by the Eq. (27).

$$V_{dc}I_{dc} = P_h - P_g \quad (27)$$

In *generating mode*, the power flows out of PHESS which increases

the DC link voltage. The PI controller in the outer loop generates current reference values to the inner loop based on the DC link voltage error. The DC link current determines the direction of power flow, when $P_h > P_g$ the DC link current I_{dc} will be positive thus aiding the power flow from PHESS to the grid. To export maximum power from the Reversible Pump Turbine to the grid, the DC link voltage has to be maintained constant [48] throughout the operation as shown in Eq. (28), where P_h is the power from the Reversible Pump Turbine and P_g is the power injected into the grid. The condition for the minimum DC link voltage is dictated by the line voltage of the grid [48]. The DC link

voltage reference is set by satisfying the condition (29). The reactive power command is set at zero to ensure no reactive power injection into the grid. The obtained values are further fed to the current controllers in the inner loop.

$$V_{dc} C \frac{dV_{dc}}{dt} = P_h - P_g \quad (28)$$

$$V_{dc} \geq 1.6 V_{GL} \quad (29)$$

In *pumping mode*, the DC link voltage reference is set different and is dictated by the rated voltage of the PMSM. Since the power is consumed by the PMSM, the DC link voltage gets reduced according to the Eq. (28). To maintain a constant DC link voltage, the power is drawn from the grid and hence the direction of power flow is reversed. During rectification operation of the GCC, the anti-parallel diodes in GCC conduct based on the firing of IGBTs which enables bidirectional power flow. The reference value of the q axis current loop is set to zero, to ensure no reactive power is drawn from the grid. Based on the DC link voltage error, the PI controller in the outer loop generates a d-axis current reference $i_{g,d}^*$ for the inner current control loops. The decoupling term is added to the control signal from the current controllers to generate the reference values of direct $U_{g,d}^*$ and quadrature axis $U_{g,q}^*$ voltages (3031).

$$U_{g,d}^* = U_{g,d} - \omega L_f + V_{g,d} \quad (30)$$

$$U_{g,q}^* = U_{g,q} + \omega L_f + V_{g,q} \quad (31)$$

The decoupling terms are introduced to eliminate the cross-coupling present in the control signal generated by the current controllers and it ensures improved dynamic performance where, L_f is the inductance of the filter coupled to the line, which is an LCL- filter in this work [49]. The synchronously rotating reference frame components ($d-q$) are converted to stationary reference frame components ($\alpha\beta$) using inverse Park's transformation. The $\alpha\beta$ components of the reference voltage are used by the SVPWM block to generate gate pulses to the switches of the GCC.

6. Results and discussion

The dual mode operation of PHESS, in pumping and generating mode is simulated in MATLAB Simulink and the results are presented in this section.

6.1. Pumping mode

The ultimate objective of the variable speed operation of PHESS in pumping mode is to achieve satisfactory pumping characteristics at part load. To justify the effectiveness of the proposed control strategy, the power input to the machine is limited between 50% and 70% of its rated power.

To maintain the specified power levels, the surplus power in the grid is varied from a minimum of 750 W to a maximum of 950 W with a step size of 100 W in each ten-second interval by appropriately switching the load which is shown in Fig.11(a). In this mode of operation, the volume of water in the reservoir and water level in the reservoir are initialized to zero, and the volume of water and the water level in the reservoir increases linearly, whose slope is decided by the water discharge rate of the pump. The slope of the reservoir volume characteristics shown in Fig.11(b) gives the discharge of pump Q in m^3/sec for the given period. The variation of the water level is presented in Fig.11(c) which is one of the critical parameters used to decide the mode of operation of the PHESS. The discharge of the pump is proportional to its power input given by Eq. (9).

The pump discharge characteristics are shown in Fig.11(d), in which the discharge of the pump varies as the power input to it is varied. As described in section 4.3, the actual rotor speed has to track the

estimated reference speed which is presented in Fig.11(e). The blue line corresponds to the actual rotor speed and the red line is the reference speed estimated by the speed control algorithm. The initial peak overshoot in speed characteristics is due to the starting dynamics of the PHESS, which settles down within one second and the rotor speed tracks the reference speed generated. The torque characteristics of PHESS in pumping is represented by Fig.11(f). The PHESS is operated in constant torque mode and speed is varied, thus controlling the power consumed by PMSM. The net load acting on the shaft is 10 N-m shown with the red line and the electromagnetic torque developed in PMSM is 13 N-m which is shown with the blue line. The difference between actual shaft torque and the developed electromagnetic torque is due to the frictional torque acting on the shaft. Ideally, the net power flow into the DC link capacitor should be zero. The condition given in Eq. (29) is satisfied by setting the reference DC link voltage to 125 V where the inverter line to line output voltage is 80 V and interfaced with the microgrid using a transformer. The constant DC link voltage response in pumping mode is shown in Fig.11(g). The direction of DC link current flow decides the power flow direction in both the modes of operation. The DC link current characteristics in pumping mode are shown in Fig.11(h) where the negative sign of the DC link current indicates the power flow from the microgrid to the PHESS. As the load changes, the DC link voltage remains constant and to maintain the power drawn by the PMSM, the DC link current is regulated by the GCC.

The surplus power in the microgrid is sensed by the MG controller and the power command is passed to the PHESS which is shown in Fig.11(i). The negative power indicates the power drawn from the microgrid and it has to track the reference power command from the microgrid controller so that the PHESS can take part in the primary, secondary controls of the microgrid. The blue line indicates the power consumed from the grid, the red line corresponds to the power command from the MG controller and the black line corresponds to the actual power input to the machine. The losses at part load operation are analysed in pumping mode, where the efficiency is calculated against the turbine input power and the power drawn from the grid. It is evident from Table 2 that the efficiency of the system increases as the power input approaches the rated value. To maintain the microgrid power balance, the actual power drawn from the grid is almost equal to the reference power input. Thus validating the control strategy in the pumping mode of operation.

6.2. Generating mode

The simulation results of PHESS operating in generating mode is presented in this section. The deficit power in the grid is varied from a minimum of 500 W to a maximum of 1000 W with a step size of 100 W by switching the loads at a time interval of 5 s. The power command signal to the PHESS is given by the MG controller which is presented in Fig.12(a). In this mode, the upper reservoir volume is initialized to its full capacity of $150 m^3$ which implicitly means the water level in the reservoir is 5 m (depth of the upper reservoir). The water level and the volume of water in the upper reservoir decreases with time as shown in Fig.12(b) and Fig.12(c). The slope of the volume characteristics of the reservoir gives the discharge of water at a particular time interval and the average discharge in 30 s is $0.00498 m^3/s$. In both the figures, the slope depends on water discharge supported by the Eq.s (3) and (5).

The discharge of water in the conduit is controlled by adjusting the

Table 2
Efficiency Analysis in Pumping Mode.

Turbine Power Input (W)	Power Drawn from the Grid (W)	Efficiency (%)
520	750	69.3
590	850	69.4
670	950	70.5

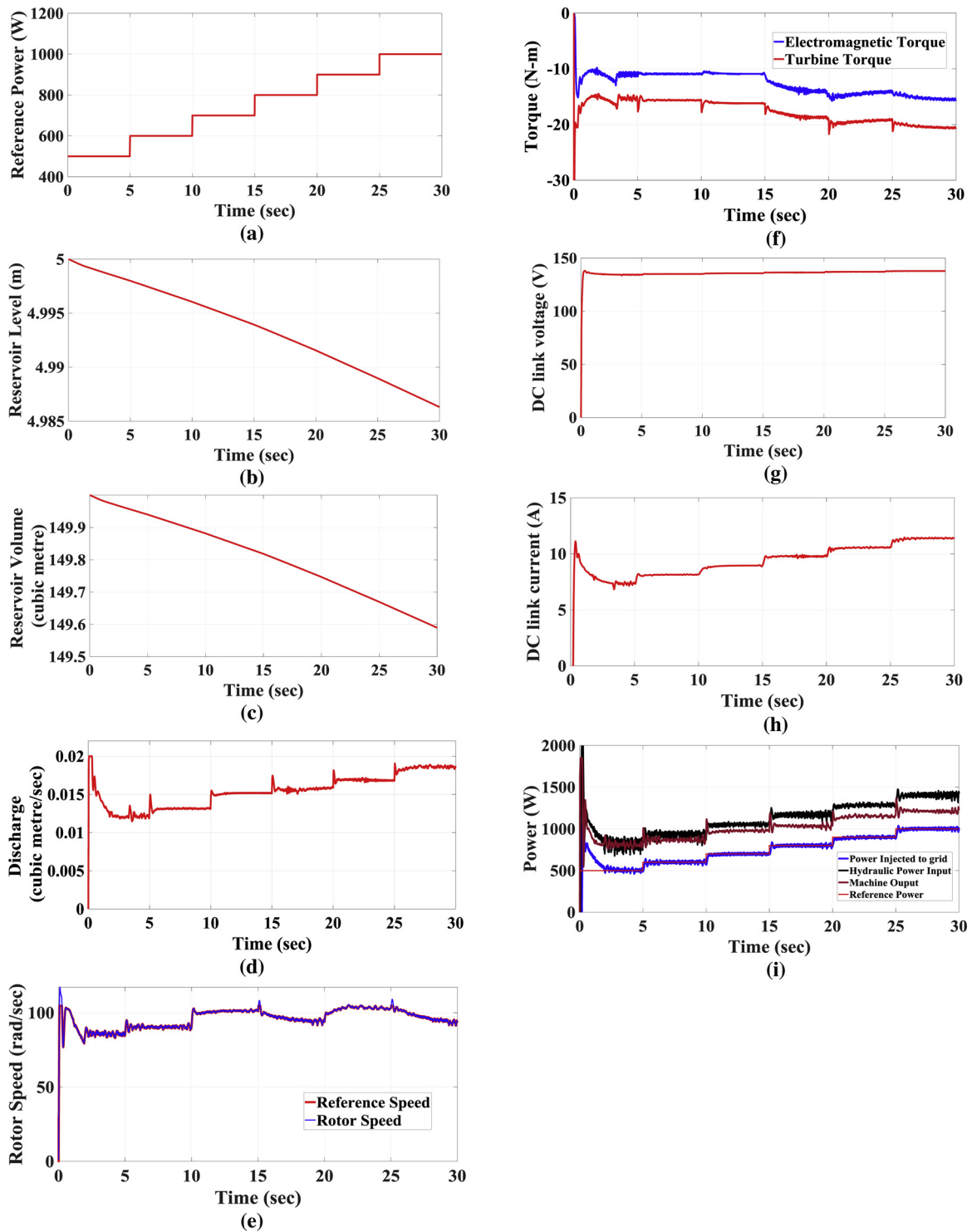


Fig. 12. Analysis of Generation Mode with the obtained simulation results: (a) Reference power command from MG controller (b) Decrease in Reservoir Volume (c) Decrease in Reservoir Level (d) Water discharged to the turbine (e) Mechanical Shaft Speed (f) Electromagnetic & Shaft Torque (g) DC link Voltage (h) DC link Current (i) Power measured at various points.

gate valve position in accordance with the power command from MG controller which is explained in section 3.3. Since the power output from PHESS is directly proportional to discharge (7), it varies proportionally to the power command signal. The water discharge characteristics are shown in Fig.12(d), the initial peak overshoot is due to sudden discharge of water to the RPT and it settles within a considerable amount of time. The discharge is limited to $0.02 \text{ m}^3/\text{s}$ to maintain the discharge limits of the turbine. The speed characteristics of PHESS

in generating mode is shown in Fig.12(e). The actual rotor speed in blue line tracks the reference speed estimated by the APO algorithm, which validates the proposed speed control algorithm in generating mode.

The torque characteristics of PHESS is shown in Fig.12(f), where the red colour is the mechanical torque acting on the shaft and blue colour curve is the developed electromagnetic torque. The torque values are negative, indicating the operation of PMSM in generating mode and there is a difference of about 3 N-m at each time interval between the

Table 3
Efficiency Analysis in Generating Mode.

Hydraulic Power Input (W)	Power Injected to the Grid (W)	Efficiency (%)
800	500	62.5
930	600	64.5
1050	700	66.6
1150	800	69.6
1280	900	70.3
1400	1000	71.4

torque values, which is due to the frictional torque acting against the shaft torque. The DC link voltage has to remain constant at 140 V as constrained by the Eq. (28) since the line to line voltage is 80 V and interfaced with the microgrid using a transformer. The actual DC link voltage settles at 135 V as shown in Fig.12(g). The DC link current has to vary as the power output from the PHESS varies, which is shown in Fig.12(h). The current is positive (20) which indicates that the power flow is from PHESS to the grid.

One of the objective in generating mode is to control the power exported to the grid and the characteristics of the same are shown in Fig.12(i). The power output from PHESS in blue line follows the reference power signal shown in red colour. The black and brown colour curves indicate the turbine and PMSM output power respectively. The initial response of the system is slow and the power starts tracking its reference once the water discharge to the turbine reaches a steady state value. The initial peak overshoot is due to the sudden discharge of water to the turbine. The power loss in the system is analysed with the difference between the net hydraulic power input to the turbine and the actual power injected to the grid and presented in Table 3. The efficiency of the system increases as the water discharge rate approaches the rated value. The reference power tracking efficiency demonstrated by the simulation results shows that the PHESS was able to generate power efficiently even at part load operation.

7. Conclusion

The main objective of the work is to model a sustainable energy storage system which exploits the existing dug well and a surface level tank at agricultural farms in rural India. The system is a downscaled version of the conventional Pumped Hydro Storage System and called as Pico Hydel Energy Storage System. Various control strategies were developed at different levels for variable speed operation of PHESS, which has a high degree of flexibility than the fixed speed PHESS. The PHESS is modelled independently of the type of renewable energy source so that it can be plugged to any microgrid with various renewable energy sources. The control strategies are optimized to accept the reference power as the command from the MG controller. The power delivered or absorbed by the PHESS is controlled by mapping the reference power input and the rotational speed of the rotor with separate strategies in both the modes of operation, which makes it a generic model to integrate it with any MG. The following conclusions are made from the proposed work.

- The mathematical model of each module of PHESS is validated by analysing the simulation results obtained with the theoretical equations and it is presented in this paper.
- In generating mode, the maximum power is extracted at all operating heads and discharge rates with the proposed adaptive perturb and observe algorithm. The efficiency of the system increases as it approaches the rated power and discharge rates. The highest efficiency of 71.4% is achieved for a power command of 1000 W.
- The relationship established between the surplus power in the microgrid and the speed of RPT in pumping mode through regression analysis has generated optimal reference speed. The operation of PHESS in pumping mode was analysed in part load conditions with

the power input of 50% to 70% of the rated power, which demonstrates the effectiveness of variable speed operation in pumping mode. The maximum pumping efficiency of 70.5% is reached with a power input of 950 W from the grid.

- The PHESS controlled by power converters provides a rapid response in both the modes of operation, unlike the mechanically controlled fixed speed system which has a slower response. The PHESS responds to change in power command and settles at the new power command within 2 s. This indicates that the proposed system has the potential to take part in various controls dictated by the microgrid controller.

Acknowledgement

This research was supported by the Long Term Research Grant (LRGS), Ministry of Education Malaysia for the program titled “Decarbonisation of Grid with an Optimal Controller and Energy Management for Energy Storage System in Microgrid Applications”.

Appendices

PMSM: Three Phase Star Connected, Salient Pole rotor. Power = 1.5 kW, Pole Pairs = 3, $L_d = 5.71$ mH, $L_q = 9.94$ mH, Resistance = 0.775Ω, flux per pole = 0.2848 Wb.

Reversible Pump Turbine: Power = 1.2 kW, Rated Head = 16–22 m, Rated Discharge = 10–16 l/s.

References

- [1] Draft National Energy Policy - India 2017, NITI Aayog, Gov. India, 2017, pp. 1–106.
- [2] Economic Survey of India 2017-2018, Government of India, Ministry of Finance, 2018.
- [3] N. Sivakumar, D. Das, N.P. Padhy, Variable speed operation of reversible pump-turbines at Kadamparai pumped storage plant - A case study, *Energy Convers. Manage.* 78 (2014) 96–104, <https://doi.org/10.1016/j.enconman.2013.10.048>.
- [4] T. Kerdpol, F.S. Rahman, Y. Mitani, M. Watanabe, S. Kufeoglu, Robust virtual inertia control of an islanded microgrid considering high penetration of renewable energy, *IEEE Access* 6 (2018) 625–636, <https://doi.org/10.1109/ACCESS.2017.2773486>.
- [5] T. Ma, H. Yang, L. Lu, Feasibility study and economic analysis of pumped hydro storage and battery storage for a renewable energy powered island, *Energy Convers. Manage.* 79 (2014) 387–397, <https://doi.org/10.1016/j.enconman.2013.12.047>.
- [6] T. Berger, Practical constraints for photovoltaic appliances in rural areas of developing countries Lessons learnt from monitoring of stand-alone systems in remote health posts of North Gondar Zone, Ethiopia, *Energy Sustain. Dev.* 40 (2017) 68–76, <https://doi.org/10.1016/j.esd.2017.07.001>.
- [7] J.K. Kaldellis, D. Zafirakis, K. Kavadias, Techno-economic comparison of energy storage systems for island autonomous electrical networks, *Renew. Sustain. Energy Rev.* 13 (2009) 378–392, <https://doi.org/10.1016/j.rser.2007.11.002>.
- [8] B.P. Hayes, A. Wilson, R. Webster, S.Z. Djokic, Comparison of two energy storage options for optimum balancing of wind farm power outputs, *IET Gener. Transm. Distrib.* 10 (2016) 832–839, <https://doi.org/10.1049/iet-gtd.2015.0486>.
- [9] A. Biswas, A. Kumar, Techno-Economic Optimization of a Stand-alone PV/PHS/Battery systems for very low load situation, *Int. J. Renew. Energy Res.-IJRER* (2017), <http://www.ijrer.org/ijrer/index.php/ijrer/article/view/4900/pdf>.
- [10] B.R. Cobb, K.V. Sharp, Impulse (Turgo and Pelton) turbine performance characteristics and their impact on pico-hydro installations, *Renew. Energy* 50 (2013) 959–964, <https://doi.org/10.1016/j.renene.2012.08.010>.
- [11] A. Poulain, J. De Dreuzey, P. Goderniaux, Pump Hydro Energy Storage systems (PHESS) in groundwater flooded quarries, *J. Hydrol. (Amst)* 559 (2018) 1002–1012, <https://doi.org/10.1016/j.jhydrol.2018.02.025>.
- [12] S.P. Koko, K. Kusakana, H.J. Vermaak, Optimal power dispatch of a grid-interactive micro-hydrokinetic-pumped hydro storage system, *J. Energy Storage.* 17 (2018) 63–72, <https://doi.org/10.1016/j.est.2018.02.013>.
- [13] T.T. Anilkumar, S.P. Simon, N.P. Padhy, Residential electricity cost minimization model through open well-pico turbine pumped storage system, *Appl. Energy* 195 (2017) 23–35, <https://doi.org/10.1016/j.apenergy.2017.03.020>.
- [14] 5th Census of Minor Irrigation Schemes Report, Government of India, Ministry of Water Resources, River Dev. Ganga Rejuvenation (2017).
- [15] Y. Pannatier, B. Kawkabani, C. Nicolet, J.J. Simond, A. Schwery, P. Allenbach, Investigation of control strategies for variable-speed pump-turbine units by using a simplified model of the converters, *IEEE Trans. Ind. Electron.* 57 (2010) 3039–3049, <https://doi.org/10.1109/TIE.2009.2037101>.
- [16] S. Nababan, E. Muljadi, F. Blaabjerg, An overview of power topologies for micro-hydro turbines, 2012 3rd IEEE Int. Symp. Power Electron. Distrib. Gener. Syst. (2012) 737–744, <https://doi.org/10.1109/PEDG.2012.6254084>.
- [17] A. Joseph, T.R. Chelliah, A review of power electronic converters for variable speed

- pumped storage plants: configurations, operational challenges, and future scopes, *IEEE J. Emerg. Sel. Top. Power Electron.* 6 (2018) 103–119, <https://doi.org/10.1109/JESTPE.2017.2707397>.
- [18] N. Osamu, H. Mikisuke, T. Kiyohito, O. Dr. Eng. Takashi, Hitachi's adjustable-speed pumped-storage system contributing to prevention of global warming osamu, *Hitachi Rev.* 59 (2010) 99–105, <https://doi.org/10.1117/12.2010100>.
- [19] S.M.H. Hosseini, M.R. Semsar, A novel technology for control of variable speed pumped storage power plant, *J. Cent. South Univ.* 23 (2016) 2008–2023, <https://doi.org/10.1007/s11771-016-3258-y>.
- [20] R. Raja Singh, T. Raj Chelliah, P. Agarwal, Power electronics in hydro electric energy systems - A review, *Renew. Sustain. Energy Rev.* 32 (2014) 944–959, <https://doi.org/10.1016/j.rser.2014.01.041>.
- [21] S. Benelghali, M.E.H. Benbouzid, J.F. Charpentier, Comparison of PMSG and DFIM for marine current turbine applications, 19th Int. Conf. Electr. Mach. ICEM 2010 (2010) 1–6, <https://doi.org/10.1109/ICELMACH.2010.5608118>.
- [22] J.A. Suul, K. Uhlen, T. Undeland, Wind power integration in isolated grids enabled by variable speed pumped storage hydropower plant, 2008 IEEE Int. Conf. Sustain. Energy Technol (2008) 399–404, <https://doi.org/10.1109/ICSET.2008.4747040>.
- [23] D. Borkowski, Maximum efficiency point tracking (MEPT) for variable speed small hydropower plant with neural network based estimation of turbine discharge, *IEEE, Trans. Energy Convers.* 32 (2017) 1090–1098, <https://doi.org/10.1109/TEC.2017.2690447>.
- [24] J.L. Márquez, M.G. Molina, J.M. Pacas, Dynamic modeling, simulation and control design of an advanced micro-hydro power plant for distributed generation applications, *Int. J. Hydrogen Energy* 35 (2010) 5772–5777, <https://doi.org/10.1016/j.ijhydene.2010.02.100>.
- [25] M.G. Molina, M. Pacas, Improved power conditioning system of micro-hydro power plant for distributed generation applications, *Proc. IEEE Int. Conf. Ind. Technol.* (2010) 1733–1738, <https://doi.org/10.1109/ICIT.2010.5472461>.
- [26] T.J. Sobczyk, W. Mazgaj, Z. Szular, T. Węgiel, Energy conversion in small water plants with variable speed PM generator, *Arch. Electr. Eng.* 60 (2011) 159–168, <https://doi.org/10.2478/v10171-011-0015-6>.
- [27] N. Phankong, S. Manmai, K. Bhumkittipich, P. Nakawiwat, Modeling of grid-connected with permanent magnet synchronous generator (PMSG) using voltage vector control, *Energy Procedia* 34 (2013) 262–272, <https://doi.org/10.1016/j.egypro.2013.06.754>.
- [28] L. Belhadji, S. Bacha, D. Roye, Modeling and control of variable-speed micro-hydro power plant based on axial-flow turbine and permanent magnet synchronous generator (MHPP-PMSG), *IECON Proc. (Industrial Electron. Conf.)* (2011) 896–901, <https://doi.org/10.1109/IECON.2011.6119429>.
- [29] L. Belhadji, S. Bacha, I. Munteanu, A. Rumeau, D. Roye, Adaptive MPPT applied to variable-speed microhydropower plant, *IEEE Trans. Energy Convers.* 28 (2013) 34–43, <https://doi.org/10.1109/TEC.2012.2220776>.
- [30] N. Maleki, A detailed comparison between FOC and DTC methods of a permanent magnet synchronous motor drive, *J. Electr. Electron. Eng.* 3 (2017) 92, <https://doi.org/10.11648/j.jeee.s.2015030201.30>.
- [31] G. Bitew, M. Han, S. Mekonnen, P. Simiyu, A variable speed pumped storage system based on droop-fed vector control strategy for grid frequency and AC-Bus voltage stability, *Electronics* 7 (2018) 108, <https://doi.org/10.3390/electronics7070108>.
- [32] B. Guo, S. Bacha, M. Alamir, A. Mohamed, C. Boudinet, LADRC applied to variable speed micro-hydro plants: experimental validation, *Control Eng. Pract.* 85 (2019) 290–298, <https://doi.org/10.1016/j.conengprac.2019.02.008>.
- [33] J. Fraile-Ardanuy, J.R. Wilhelmi, J.J. Fraile-Mora, J.I. Pérez, Variable-speed hydro generation: operational aspects and control, *IEEE Trans. Energy Convers.* 21 (2006) 569–574, <https://doi.org/10.1109/TEC.2005.858084>.
- [34] S. Nag, K.Y. Lee, DFIM-based variable speed operation of pump-turbines for efficiency improvement, *IFAC-PapersOnLine.* 51 (2018) 708–713, <https://doi.org/10.1016/j.ifacol.2018.11.788>.
- [35] H.J. Fard, H.R. Najafi, H. Eliahi, Novel design and simulation of predictive power controller for a doubly-fed induction generator using rotor current in a micro-hydro power plant, *Energy Equip. Syst.* 5 (2017) 43–58.
- [36] T. Poompavai, M. Kowsalya, Control and energy management strategies applied for solar photovoltaic and wind energy fed water pumping system: a review, *Renew. Sustain. Energy Rev.* 107 (2019) 108–122, <https://doi.org/10.1016/j.rser.2019.02.023>.
- [37] C. Serir, D. Rekioua, N. Mezzai, S. Bacha, Supervisor control and optimization of multi-sources pumping system with battery storage, *Int. J. Hydrogen Energy* 41 (2016) 20974–20986, <https://doi.org/10.1016/j.ijhydene.2016.05.096>.
- [38] A. Khiareddine, C. Ben Salah, M.F. Mimouni, Power management of a photovoltaic/battery pumping system in agricultural experiment station, *Sol. Energy* 112 (2015) 319–338, <https://doi.org/10.1016/j.solener.2014.11.020>.
- [39] A. Khiareddine, Determination of the target speed corresponding to the optimum functioning of a photovoltaic system pumping and regulation of the water level, 2013 Int. Conf. Electr. Eng. Softw. Appl. (2013) 1–5, <https://doi.org/10.1109/ICEESA.2013.6578434> (n.d.).
- [40] A. Ghosh, S. Ganesh Malla, C. Narayan Bhende, Small-signal modelling and control of photovoltaic based water pumping system, *ISA Trans.* 57 (2015) 382–389, <https://doi.org/10.1016/j.isatra.2015.01.008>.
- [41] A.R. Simpson, A. Marchi, Evaluating the approximation of the affinity laws and improving the efficiency estimate for variable speed pumps, *J. Hydraul. Eng.* 139 (2013) 1314–1317, [https://doi.org/10.1061/\(asce\)hy.1943-7900.0000776](https://doi.org/10.1061/(asce)hy.1943-7900.0000776).
- [42] S.J. Williamson, B.H. Stark, J.D. Booker, Low head pico hydro turbine selection using a multi-criteria analysis, *Renew. Energy* 61 (2014) 43–50, <https://doi.org/10.1016/j.renene.2012.06.020>.
- [43] A. Morabito, P. Hendrick, Pump as turbine applied to micro energy storage and smart water grids: A case study, *Appl. Energy* 241 (2019) 567–579, <https://doi.org/10.1016/j.apenergy.2019.03.018>.
- [44] B. Guo, A. Mohamed, S. Bacha, M. Alamir, Variable speed micro-hydro power plant: Modelling, losses analysis, and experiment validation, *Proc. IEEE Int. Conf. Ind. Technol.*, IEEE (2018) 1079–1084, <https://doi.org/10.1109/ICIT.2018.8352328>.
- [45] M.A. Abdullah, A.H.M. Yatim, C.W. Tan, R. Saidur, A review of maximum power point tracking algorithms for wind energy systems, *Renew. Sustain. Energy Rev.* 16 (2012) 3220–3227, <https://doi.org/10.1016/j.rser.2012.02.016>.
- [46] E. Muljadi, M. Singh, V. Gevorgian, M. Mohanpurkar, R. Hovsapian, V. Koritarov, Dynamic modeling of adjustable-speed pumped storage hydropower plant, *IEEE Power Energy Soc. Gen. Meet. 2015-Sept* (2015), <https://doi.org/10.1109/PESGM.2015.7286214>.
- [47] F. Blaabjerg, R. Teodorescu, M. Liserre, A.V. Timbus, Overview of control and grid synchronization for distributed power generation systems, *IEEE Trans. Ind. Electron.* 53 (2006) 1398–1409, <https://doi.org/10.1109/TIE.2006.881997>.
- [48] A.H. Kasem Alaboudy, A.A. Daoud, S.S. Desouky, A.A. Salem, Converter controls and flicker study of PMSG-based grid connected wind turbines, *Ain Shams Eng. J.* 4 (2013) 75–91, <https://doi.org/10.1016/j.asej.2012.06.002>.
- [49] M. Liserre, F. Blaabjerg, S. Hansen, Design and control of an LCL-filter-based three-phase active rectifier, *IEEE Trans. Ind. Appl.* 41 (2005) 1281–1291, <https://doi.org/10.1109/TIA.2005.853373>.